Accuracy of the Spectral and Radiometric Laboratory Calibration of the Airborne Visible/Infrared Imaging Spectrometer (AVIRIS)

Thomas G. Chrien, Robert O. Green and
Michael L. Eastwood

Jet Propulsion Laboratory, California Institute of Technology
4800 Oak Grove Drive, Pasadena, California 91109

ABSTRACT

Current research with data collected by AVIRIS includes the disciplines of ecology, geology, oceanography, inland waters, snow hydrology, and atmospheric science. In these investigations, physical parameters are calculated from AVIRIS-measured radiance spectra. AVIRIS measures the total incident radiance in 224 channels with nominally 10-nm widths between 400 and 2450 nm in the electromagnetic spectrum. Image dimensions are 10.5 km wide by 10 to 100 km in length with nominally 20- by 20-m spatial resolution. Calibration is prerequisite for extraction of quantitative information from AVIRIS data with known accuracy and precision. The spectral channel sampling interval and spectral response functions are determined with calculated accuracy for each AVIRIS channel. AVIRIS radiometric calibration coefficients, vignetting correction, instrument stability, and noise equivalent delta radiance determinations are generated. Emphasis is placed on referencing the calibration standards, procedures, and accuracy of the calibration. Future plans for improved calibration of AVIRIS in the laboratory and for using an improved onboard calibrator are discussed.

1.0 INTRODUCTION

AVIRIS is an airborne sensor that measures high spatial resolution image data of the earth in 224 spectral channels in four spectrometers (A,B,C, and D) covering the range from 400 to 2450 nm[1,2]. These data are spectrally and radiometrically calibrated. This paper describes the laboratory procedures, algorithms, measurements, and uncertainties associated with generation of the spectral and radiometric calibration.

Calibration of AVIRIS was initially reported in 1987 by Vane[3]. Since that time, improvements have been incorporated in the calibration procedure. These improvements have been primarily in the areas of increased accuracy of the transfer of calibration from standard sources, the quantification of associated accuracy, and the algorithms used to generate AVIRIS calibration files. AVIRIS system performance has been improved significantly since 1987, as reported in a companion paper by Porter[4]. These improvements, particularly with respect to stability and signal-to-noise ratio, greatly facilitate the task of instrument calibration.

Verification of the laboratory calibration is determined through an in-flight calibration experiment reported by Green et al[5]. The spectral calibration of AVIRIS agrees with the in-flight data to within 2 nm. The absolute radiometric calibration is consistent with the in-flight verification to 10 percent over the spectral range. In-flight radiometric stability, as measured by five consecutive passes over the surface calibration site, is reported to be between 3 and 5 percent. In-flight determination of AVIRIS noise equivalent delta radiance also agrees with the laboratory calibration result.

2.0 SPECTRAL CALIBRATION

The objective of the spectral calibration of AVIRIS is to determine the spectral sampling interval and spectral response function for each of the 224 channels. Variation in the spectral calibration is a consequence of the optimization of the throughput during realignment of the detector array, following a period of engineering. Realignment of the spectrometers can normally return center wavelength to within 5 nm of the previous calibration and full width at half maximum (FWHM) to within 2 nm.

The procedure for performing a spectral calibration of AVIRIS involves the following steps: (1) calibration of the laboratory monochromator from a spectral emission line source, (2) use of the monochromator to scan a narrow band source across selected AVIRIS channels while measuring the response of the channels, (3) fitting the measured responses to a Gaussian spectral response function, (4) inferring the spectral channel positions and response functions of the remaining channels, (5) quantifying and reporting the accuracy associated with these procedures.

2.1 Monochromator Calibration

The narrow band spectral calibration source consists of a Jarrell-Ash model 82-487 monochromator illuminated with a dc-stabilized lamp. The bandwidth of the monochromator is determined by the 270-mm focal length, the entrance and

exit slit widths, and the lines per millimeter grating frequency as shown in Table 1. Three monochromator configurations are used to cover the range of AVIRIS spectral channels. Each configuration uses a grating that has a blaze wavelength intended to maximize throughput. The blaze wavelengths are 0.5, 1.0, and 2.0 μm, respectively.

Table 1. Monochromator Parameters.

Spectrometer and spectral range (nm)	Grating freq. (lines/mm)	Entrance/exit slit widths (μm)	FWHM band-width (nm)
A 400 – 700	600	100	1.2
B,C 700 – 1800	600	100	1.2
D 1800 – 2500	300	50	1.2

Table 2. Effective wavelengths of mercury emission lines used for monochromator spectral calibration.

Color	Wavelength (nm)	Order	Effective Wavelength (nm)
Purple	404.656	2	809.312
		3	1213.968
		4	1618.624
		5	2023.280
		6	2427.936
Blue	435.835	2	871.670
		3	1307.505
		4	1743.340
		5	2179.175
Green	546.074	2	1092.148
		3	1638.222
		4	2184.296
Yellow1	576.959	2	1153.918
		3	1730.877
		4	2307.836
Yellow2	579.065	2	1158.130
		3	1737.195
		4	2316.260

A low-pressure mercury vapor lamp (UVP Inc. P/N 90 0012 01, S/N 243747) placed at the entrance slit is used to calibrate the monochromator. The grating drive is advanced to a position that maximizes the light throughput of a spectral emission line, as determined by visual observation. Backlash problems are avoided by always approaching a line from a shorter wavelength. Higher orders of visible lines are used to calibrate the infrared portion of the spectrum. The effective wavelength of the higher order lines is computed as shown in Table 2 by multiplying the visible wavelength times the spectral order. The counter position of each effective order is recorded at least six times and a sample variance is computed.

The monochromator calibration is computed by forming a linear fit between the effective wavelengths of observed mercury emission lines and the numeric counter. The fit uses a technique described by Bevington[6] to compute the uncertainty of the fit parameters using the uncertainties in counter position. Uncertainties in the counter position are taken to be the larger of the sample variance or the half width at half maximum (HWHM) of the monochromator bandpass in counter units. The variance in counter position is dominant in the 400- to 700-, and 700- to 1800-nm configurations. The HWHM is the greater contribution to counter uncertainty for the 1800- to 2500-nm configuration. The stated uncertainties in the positions of the spectral lines (+ or - 0.001 nm) shown in Table 2 are negligible in comparison to the counter uncertainty.

The difference from fit is shown in Figure 1. It is apparent that a higher order polynomial might lead to a better fit. This effect is due to a slight misalignment of the sine bar mechanism that drives the grating angle. This effect can be

minimized by limiting the wavelength range of the fit. A chi-squared-per-degree freedom test is performed to confirm that the fit is valid within stated uncertainty. The resultant fitting parameters for the three monochromator calibrations are given in Table 3. The increase of uncertainty for the 1800- to 2500-nm calibration is caused, in part, by the lesser resolution of the grating (300 lines per millimeter compared to 600 lines per millimeter for the other two configurations).

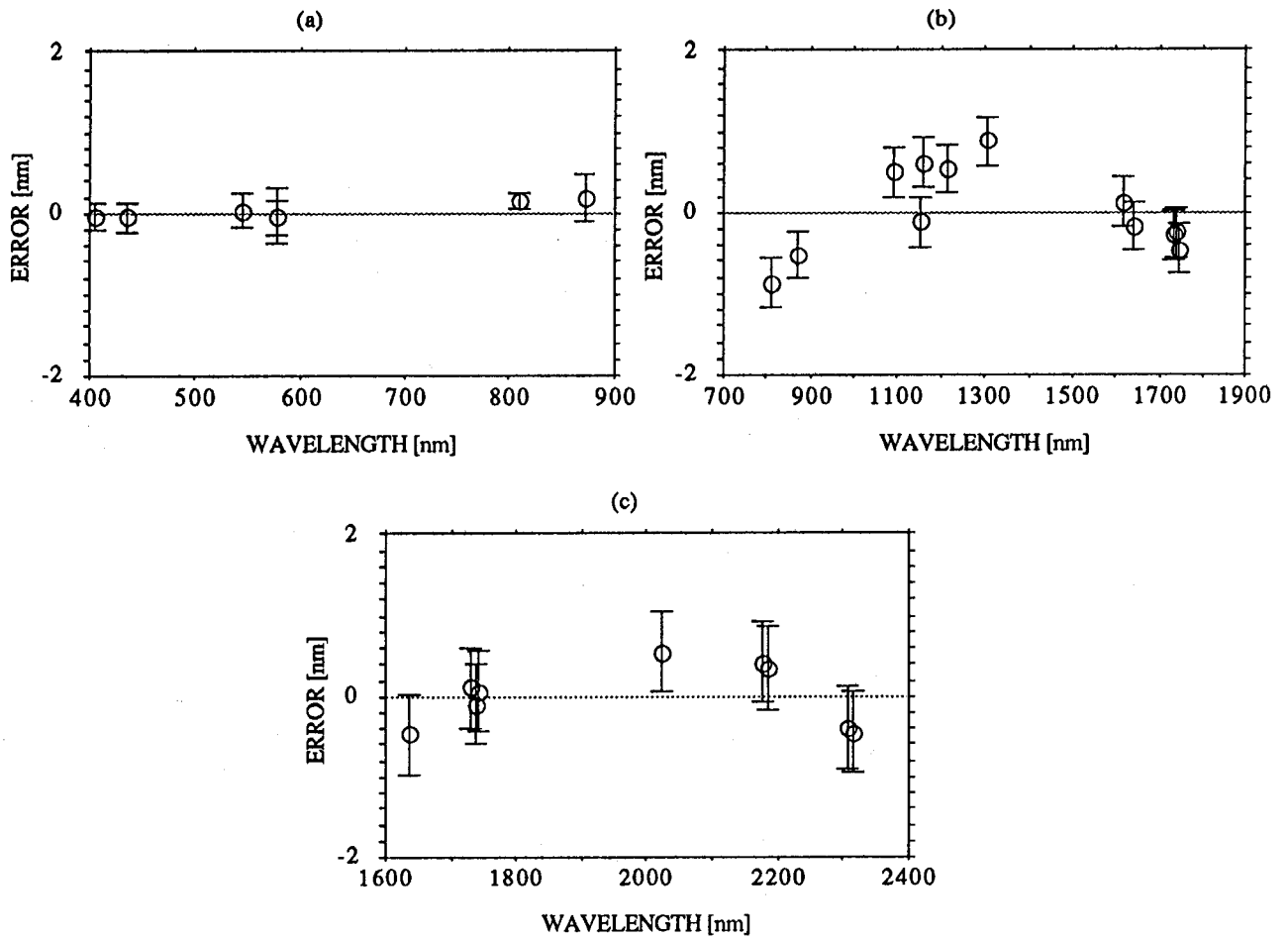

Figure 1. Difference of wavelength fit versus wavelength along with uncertainty in position for the (a) A spectrometer, (b) B and C spectrometer, and (c) D spectrometer configurations.

Table 3. Monochromator Calibration Fitting Parameters.

Spectrometer and valid spectral range (nm)	Least squares linear fit and uncertainty (nm)	Chi-squared per degree of freedom
A 400 – 700	λ = (1.99 ± 0.0005)*counter - (2.9 ± 0.2)	0.72
B,C 700 – 1800	λ = (2.00 ± 0.0001)*counter - (8.8 ± 0.1)	0.92
D 1800 – 2450	λ = (3.99 ± 0.0019)*counter - (9.8 ± 1.0)	1.02

2.2 AVIRIS Spectral Calibration Procedure

The spectral calibration stimulus shown in Figure 2 consists of the monochromator, a SORL f/4, a 1-m focal length collimator, a tungsten halogen lamp, and an Oriel dc-regulated power supply, model 68735. After calibration for a given wavelength range and configuration, the monochromator is placed so that the exit slit is located in the focal place of the collimator. The lamp is imaged onto the entrance slit of the monochromator and aligned so that the grating of the monochromator is uniformly illuminated. The entire assembly is mounted in a rack with wheels so that it can be rolled under AVIRIS, which is raised on jack stands.

Alignment of the stimulus to AVIRIS is begun by setting the grating to the zero order position and removing the slits. The output beam of the stimulus is centered on the foreoptics aperture. Jack screws placed under three corners of the rack are adjusted to maximize the peak signal of a cross-track scan. This process is repeated with a series of slits of decreasing width until the optimum angular alignment is achieved with the desired slits.

The spectral response of a channel is measured by incrementing the output wavelength counter of the monochromator in steps which correspond to 2-nm intervals. The peak signal of the cross-track scan is recorded for that channel over a 40-nm range centered about the peak signal wavelength. This process is repeated for a minimum of six channels in each of the four AVIRIS spectrometers.

2.3 Results of Spectral Calibration

The spectral response function of each of the 224 AVIRIS channels has a nominal Gaussian shape[7]. A Gaussian fitting routine, written by Sobel[8], is used to fit the response data in digitized numbers (DN) to obtain a center wavelength, full width at half maximum as shown in Figure 3. The solid line represents the best-fit Gaussian function and the squares represent measured data points. Horizontal error bars indicate the wavelength uncertainty, while the vertical error bars represent the signal response uncertainty. This is computed as the root sum square (RSS) of the product of wavelength uncertainty times the slope of the Gaussian at that point and the averaged signal variance. "Goodness" of fit is determined using chi-square-per-degree freedom analysis. The uncertainty of the fit parameters is determined by increasing the parameter until the chi-square value increases by one. In this way, computed uncertainties can be assigned to center wavelength and FWHM bandwidth. The 100 DN bias shown in the plot is due to the dark current which is not subtracted in this analysis. This bias is accounted for as one of the fitting parameters in the Gaussian routine.

Preliminary results of the chi-squared-per-degree freedom of the spectral response function curve fit show that wavelength uncertainty from the monochromator calibration is well correlated across a given spectral scan. Consequently, while the curve fit is of high precision, the absolute accuracy of the center wavelength value is limited by the monochromator calibration.

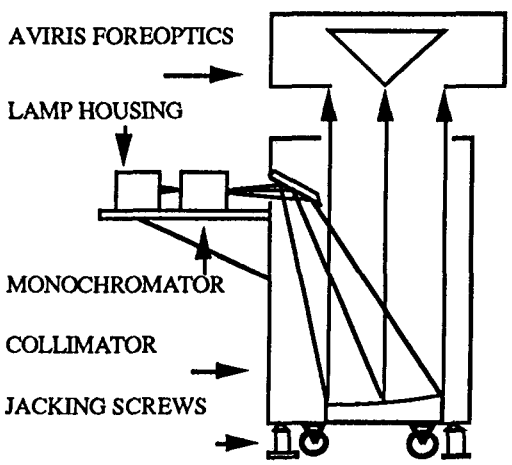

Figure 2. Spectral calibration stimulus alignment under AVIRIS.

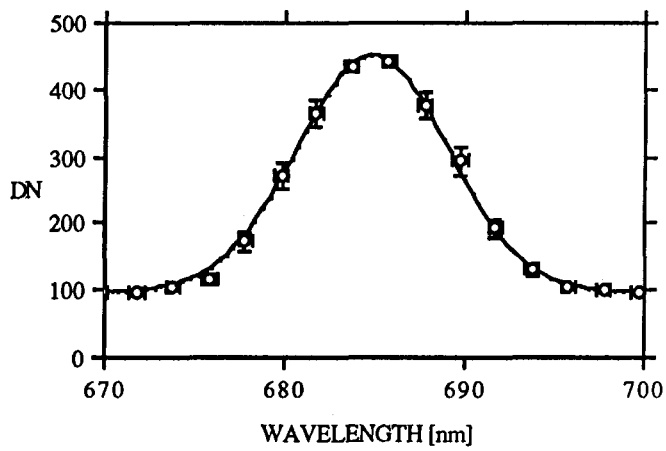

Figure 3. Spectral response function of channel A030.

AVIRIS spectral calibration is determined by computing a least squares linear fit to the measured spectral channel positions and spectral response functions. From this fit, the spectral calibration of all 224 channels is interpolated. Accuracy of the interpolated bands is computed using the procedure discussed earlier. Figure 4 shows the residual wavelength error after the linear fit is applied to the data from spectrometers A, B, C, and D. The error bars represent uncertainty in wavelength of the measured channels as limited by the monochromator calibration. The maximum residual error in the linear fit bounds the accuracy of the fit to unmeasured channels.

3.0 RADIOMETRIC CALIBRATION

Calibration parameters determined through AVIRIS radiometric calibration are: radiometric calibration coefficients, cross-track vignetting corrections, stability estimates, and noise equivalent delta radiance estimates. These calibration

parameters are calculated from AVIRIS data measured over a radiometrically and spectrally calibrated stable integrating sphere. The primary result of radiometric calibration is a file of 137,536 coefficients which calibrate AVIRIS measured DN in 224 channels to units of total spectral radiance corrected for cross-track vignetting.

Performing the radiometric calibration involves the following steps: (1) calibration of the integrating sphere with an irradiance standard, (2) measurement of the AVIRIS instrument DN from the calibrated integrating sphere, (3) computation of the calibration parameters, and (4) calculation of the accuracy.

3.1 Calibration of Integrating Sphere

The radiometric calibration stimulus is a Labsphere 100-cm-diameter integrating sphere with a 40-cm aperture. The sphere is coated internally with barium sulfate paint and illuminated with four, 500-W tungsten halogen lamps. The sphere is calibrated by establishing the ratio between the output of the sphere and a known radiance standard. The radiance standard consists of a lambertian target of known reflectance illuminated by a standard irradiance source at a fixed distance.

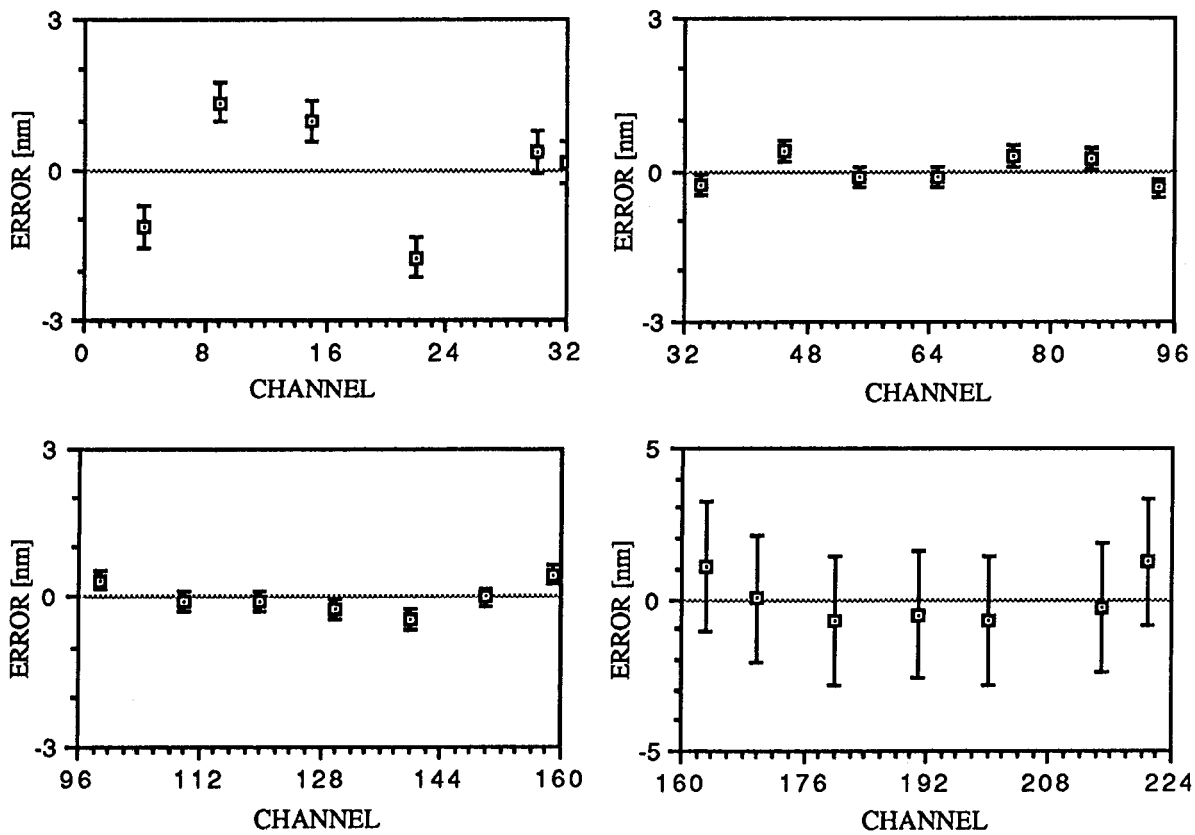

Figure 4. Plots of the residual wavelength error versus channel for the four spectrometers with error bars derived from maximum monochromator calibration uncertainty.

The irradiance standard is an Optronics model 200C, 1000-W, quartz-halogen, tungsten, coiled-coil, filament lamp (S/N S-694) powered by an Optronics model 83 constant current supply. The lamp is purchased along with a calibration report[9] which is based on the National Bureau of Standards (NBS) 1973, 1986, and 1963 scales of spectral irradiance. Irradiance values given are interpolated to the AVIRIS channel wavelengths with a spline function as shown in Figure 5. Uncertainty in irradiance, shown in Table 4, is taken to be the RSS combination of the stated NBS uncertainty, the transfer uncertainty, and the uncertainty due to a 0.1-percent fluctuation in the 8.00-A current supplied to the lamp.

Table 4. Uncertainty of irradiance standard for various wavelengths.

Wavelength (nm)	NBS Uncertainty %	Transfer Uncertainty %	Current Uncertainty %	RSS % irradiance uncertainty
500	1.18	0.55	0.4	1.4
1000	1.34	0.5	0.35	1.5
1500	1.58	0.5	0.17	1.7
2000	3.29	0.75	0.14	3.4

The reflectance standard is a Labsphere model SRT-99-100 (S/N 2432-D) Spectralon panel. Unlike pressed halon powder, this reflectance panel is easily cleaned and maintained and may be oriented vertically with little risk. A calibration certification[10] is distributed with the panel which lists the 8-deg/hemispherical spectral reflectance factor at 50-nm intervals between the range of 250 to 2500 nm, as measured using an NBS integrating sphere reflectometer. The reflectometer is calibrated using NBS standard reference material 2019a and 2021 ceramic tiles. This reflectance factor is splined to the AVIRIS wavelengths, as shown in Figure 6. Uncertainty in these measurements is given to be 0.5-percent reflectance as provided in the certification.

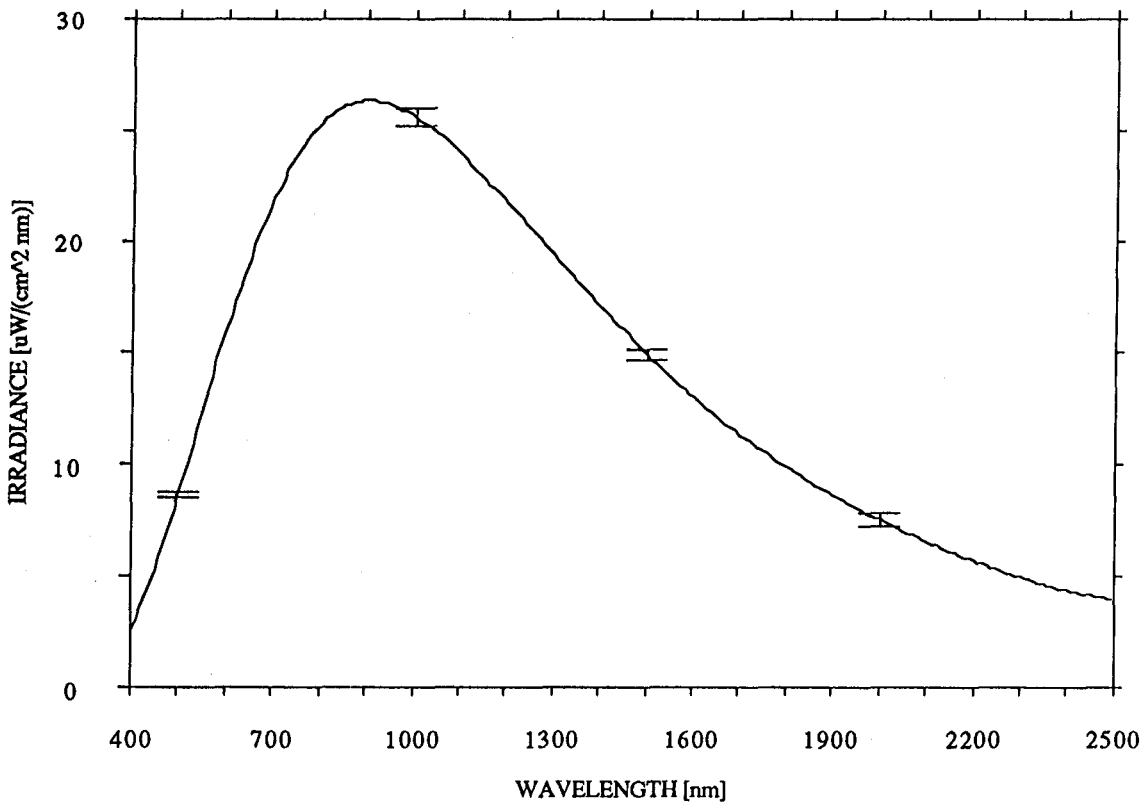

Figure 5. Spectral irradiance of standard lamp as a function of wavelength.

The radiance target geometry is shown in Figure 7. The lamp is located along a line normal to the center of the Spectralon panel at a distance of 50 ± 0.1 cm. The spectral radiance of the target is computed using Equation 1.

$$L(\lambda)=\frac{E(\lambda)R(\lambda)}{\pi} \tag{1}$$

$L(\lambda)$ is the spectral radiance as viewed by the spectroradiometer, $E(\lambda)$ is the lamp irradiance at a distance of 50 cm and $R(\lambda)$ is the reflectance of the reflectance panel. Uncertainty in the absolute radiance of the target is computed using error propagation in equation (1). These uncertainties are given in Table 5. The target spectral radiance is shown in Figure 8, along with the uncertainty in radiance.

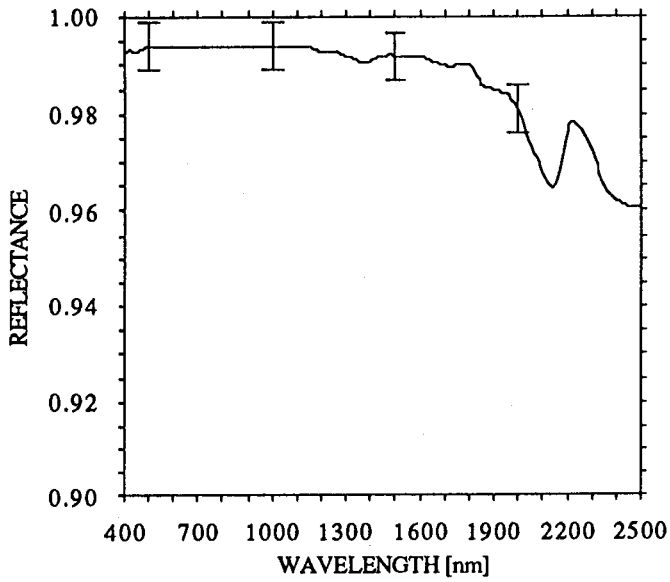

Figure 6. Spectralon 8-deg/hemispherical spectral reflectance factor.

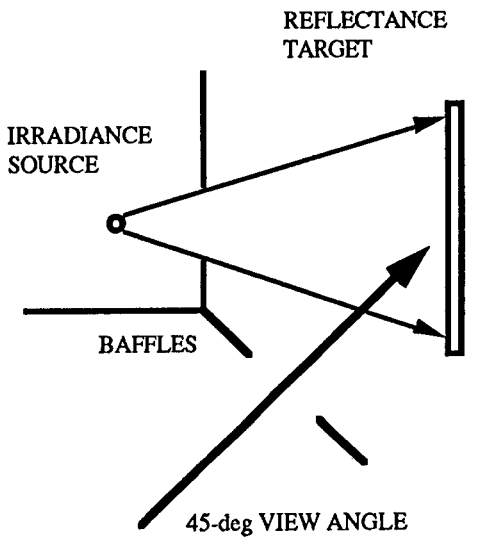

Figure 7. Radiance target geometry.

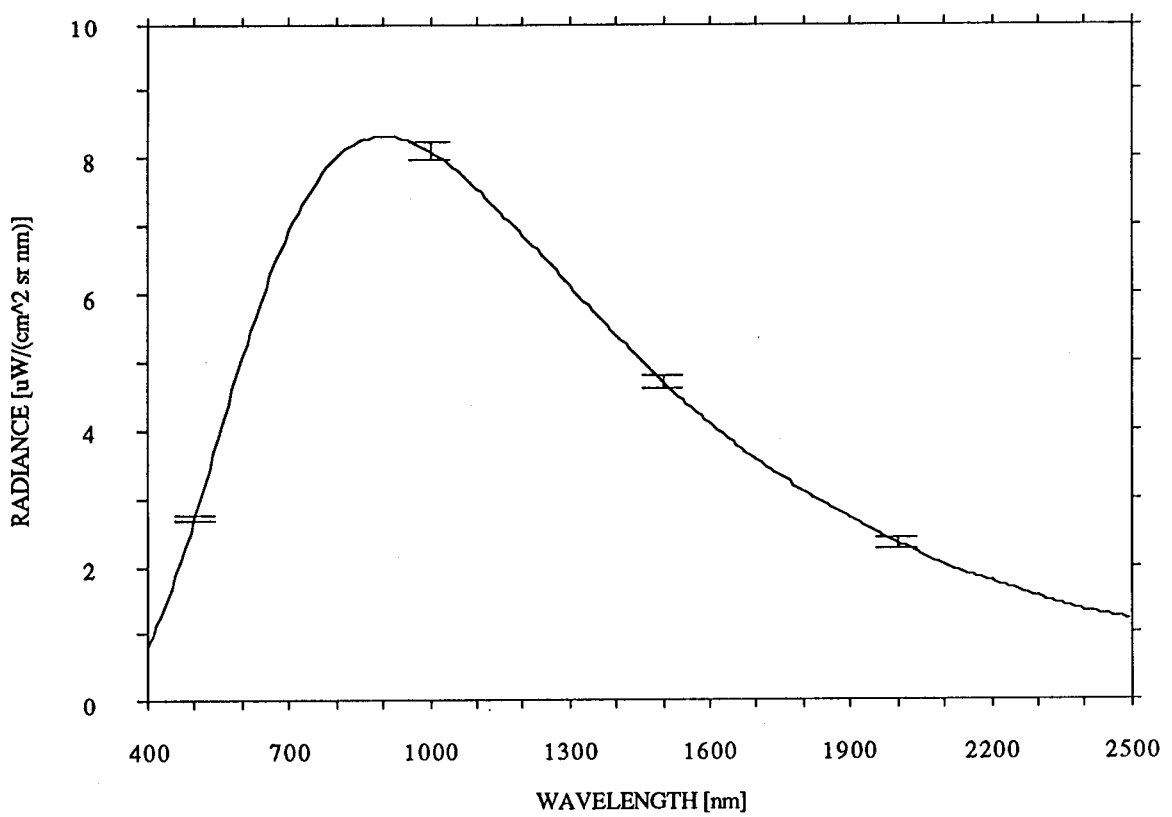

Figure 8. Radiance target spectral radiance as a function of wavelength.

Table 5. Uncertainty of radiance target for various wavelengths.

Wavelength (nm)	Irradiance uncertainty %	Reflectance uncertainty %	Distance uncertainty %	RSS uncertainty %
500	1.36	0.5	0.4	1.50
1000	1.47	0.5	0.4	1.61
1500	1.67	0.5	0.4	1.78
2000	3.38	0.5	0.4	3.44
2500	6.58	0.5	0.4	6.61

3.2 Calibration of the Integrating Sphere

Transfer of radiance calibration from the reference to the integrating sphere stimulus is accomplished using a GER IRIS single-field-of-view portable spectroradiometer[11] (S/N JPL-1017.) This spectroradiometer has been modified to provide improved spectral calibration repeatability, data acquisition rate, radiometric stability, and signal-to-noise ratio. For the integrating sphere calibration, the spectroradiometer alternately views the standard radiance target and the integrating sphere over a 5-minute period. The mean ratio of the signal between the two sources is splined to the AVIRIS channel wavelengths, and then multiplied by the spectral radiance of the reference target to determine the spectral radiance of the integrating sphere.

Spectral calibration of the spectroradiometer is performed by recording the spectrum of low pressure krypton emission line lamp. A third-order polynomial is fit between the krypton lines and spectroradiometer channels for each grating to provide a spectral calibration over the 400- to 2450-nm range. Consecutive spectra acquired of the krypton lamp are shown to have less than 1.0-nm spectral calibration error. Both the spectral channel sampling interval and spectral response function FWHM of the spectroradiometer are less than that of AVIRIS. Accuracy of the transfer of radiance from the standard illuminated reference panel to the integrating sphere with the spectroradiometer is shown to be 0.5 percent. This accuracy is determined as the root-mean-squared deviation divided by the mean of five consecutive integrating spheres to radiance standard ratio measurement.

The absorption features and steep slopes present in the integrating sphere as shown in Figure 9 require that this spectrum be measured at a spectral resolution better than AVIRIS. This spectrum is then convolved with the AVIRIS spectral channel positions and response functions FWHM to provide the basis for absolute radiometric calibration. The absorption features at 1400 and 1900 nm are caused by adsorbed water. To eliminate the effect of these features on the calibration, the integrating sphere is warmed up 1 hour prior to calibration. In addition, calibration data for the integrating sphere and AVIRIS illuminated by the integrating sphere are acquired concurrently.

At the time of calibration, the radiance output of the sphere is measured continuously using a broadband, stable silicon photodetector. The results of this monitoring show the sphere/detector combination is stable to better than 1 percent.

Total accuracy of the sphere radiance calibration is determined as the root sum square of the uncertainty in the radiance of the reference source, uncertainty in the transfer of calibration to the sphere including the uncertainty of the spectral calibration of the spectroradiometer, and the stability of the integrating sphere. These uncertainties are shown in Table 6.

Radiometric calibration of AVIRIS proceeds by establishing the stability, the cross-track vignetting corrections, the radiometric calibration coefficients, and the noise-equivalent delta radiance for the 224 spectral channels.

Stability is determined, following a 1-hour instrument and integrating sphere warm-up, through acquisition of 1-minute data sets every half hour over a period of 4 hours. The average of each of these 1-minute samples is formed for the central cross-track sample of each channel for 512 image lines to provide an accurate estimate of the sample mean. From these sample means, the minimum, maximum, and mean DN with dark current subtracted over the 4-hour period are determined. Figure 10 shows the laboratory stability determined as the maximum-minimum divided by the mean for the laboratory calibration. This worst-case analysis shows that most of the AVIRIS spectral channels are stable to better than 3 percent during the 4-hour laboratory calibration period.

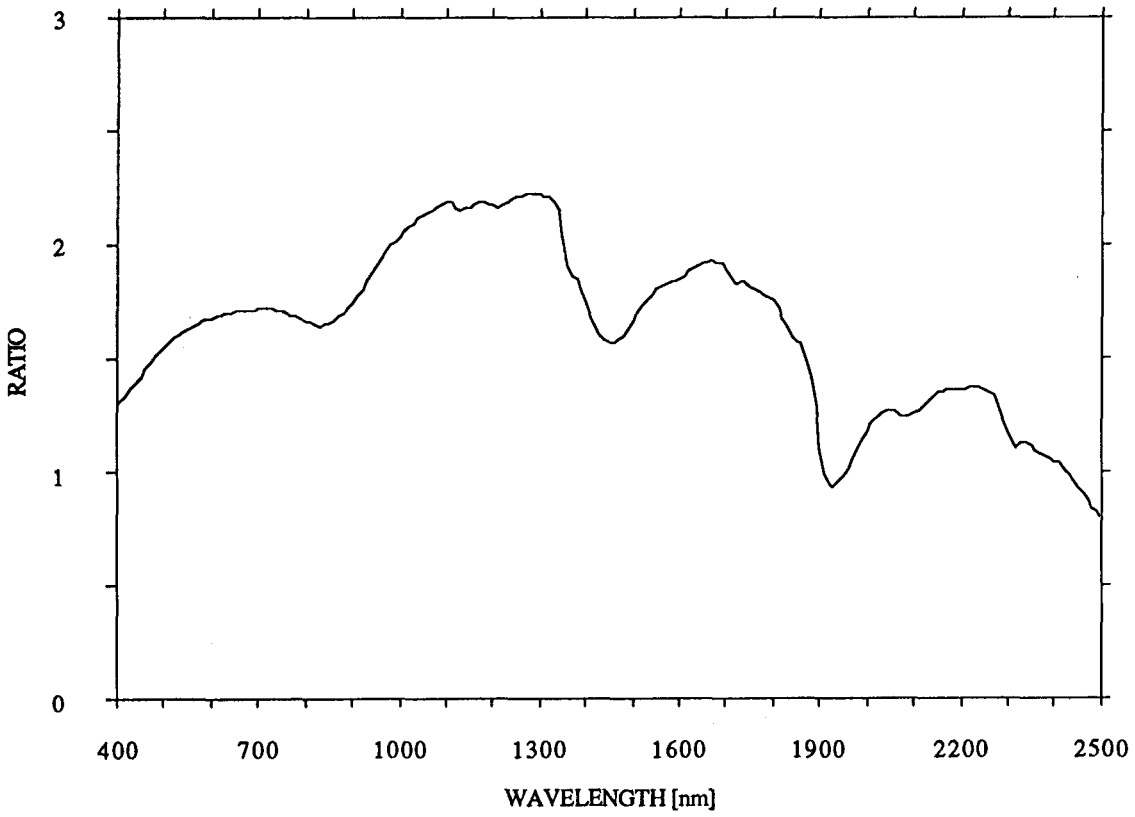

Figure 9. Ratio of the integrating sphere spectral radiance to the target as measured by the GER spectroradiometer.

Table 6. Accuracy of integrating sphere radiance.

Wavelength (nm)	Target uncertainty %	Transfer uncertainty %	Sphere stability %	RSS uncertainty %
500	1.50	0.5	1.0	1.87
1000	1.61	0.5	1.0	1.96
1500	1.78	0.5	1.0	2.10
2000	3.44	0.5	1.0	3.62

3.3 Radiometric Calibration of AVIRIS

Vignetting corrections are calculated for the 224 channels through formation of the mean for 512 lines of image for all cross-track samples. From these data, the dark current is subtracted and each cross-track sample normalized to central cross-track sample. The normalized vignetting profile for the central channel in the AVIRIS B spectrometer is given in Figure 11. Toward the edges of the field of view, vignetting accounts for roughly a 4-percent loss in signal. Calibration coefficients to compensate for vignetting are calculated as the inverse of the vignetting profile for each spectral channel.

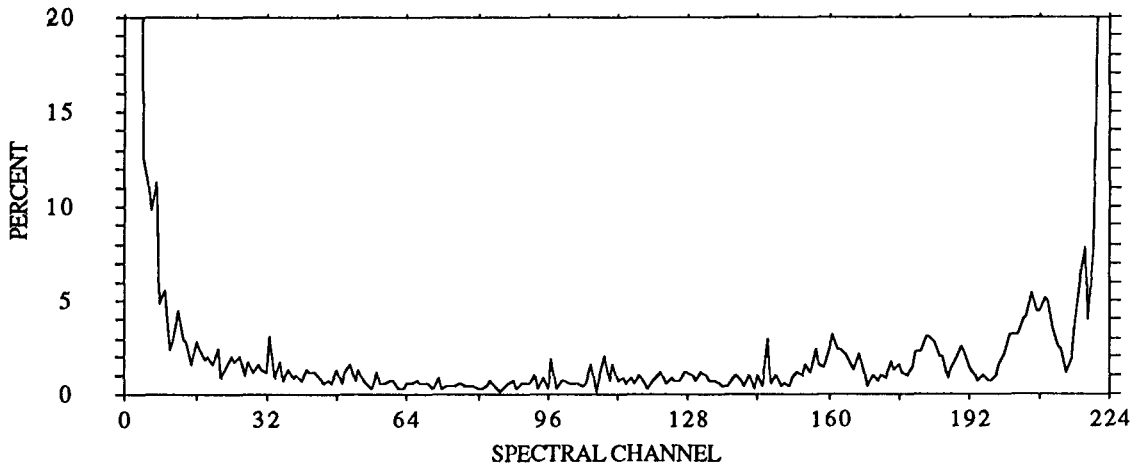

Figure 10. The percent stability of AVIRIS in the laboratory over a 4-hour period.

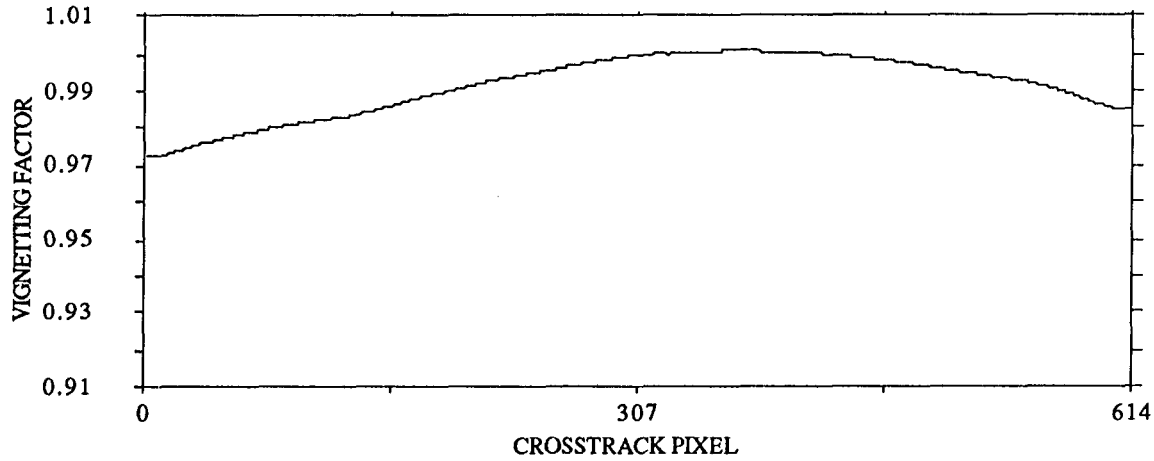

Figure 11. Cross-track vignetting for the central channel of the AVIRIS B spectrometer.

Radiometric calibration coefficients are determined by calculating the ratio of integrating sphere radiance to the mean of AVIRIS dark current subtracted DN acquired over the integrating sphere for the central cross-track sample. These coefficients calibrate AVIRIS reported DN with dark current subtracted to total spectral radiance.

In the laboratory, noise-equivalent delta radiance is calculated to place a precision calibration on AVIRIS-measured data. This quantity is calculated as the root-mean-squared deviation of 100 calibrated radiance spectra measured over the stable integrating sphere. Figure 12 presents the AVIRIS noise-equivalent radiance calculated in the laboratory. The downward-going spikes at channels 33, 97, and 161 are the first channels in spectrometers B, C, and D, respectively, and are not used. The upward-going spikes are the result of noisy detector elements in the C spectrometer array, which has subsequently been replaced.

4.0 CALIBRATION OF AVIRIS DATA

AVIRIS data are calibrated at two levels. First, the DN reported by AVIRIS are corrected for dark current, vignetting, and detector read-out-delay and calibrated to units of total spectral radiance. Second, all determined spectral, radiometric, and geometric characteristics as calculated accuracies and precisions are reported with the data or through publications.

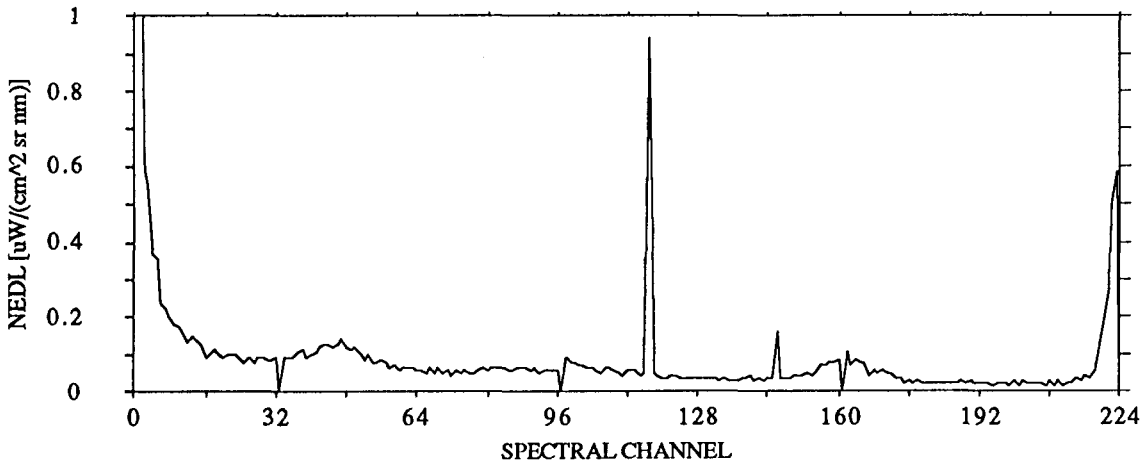

Figure 12. NEΔL

Calibration of the measured AVIRIS data begins with subtraction of the dark current measured at the end of each image line. A mean of 101 lines of dark current is used to suppress introduction of noise present in the dark-current measurements. Following dark-current subtraction, the cross-track vignetting is compensated. Radiometric calibration coefficient are multiplied against the DN calibrating the data to units of total spectral radiance. Finally, the detector read-out-delay is compensated through a minor spatial resampling of less than one sample in the cross-track direction. These procedures were described initially by Reimer[12], and a more current description is provided by Larson[13]. The measured dark current, vignetting, and radiometric calibration coefficients are provided with each distributed AVIRIS image.

Spectral calibration is reported with each AVIRIS image as the spectral channel position, and response function FWHM for the 224 channels. Absolute radiometric accuracy, stability, and other radiometric parameters are provided in AVIRIS calibration publications. Precision is provided as the noise equivalent delta radiance determined for each AVIRIS image and included with the data. Geometric calibration of AVIRIS is provided through periodically reporting the spatial properties measured in the laboratory.

5.0 ACCURACY OF AVIRIS CALIBRATION

5.1 Accuracy of the Spectral Calibration

While the original AVIRIS functional requirements document specifies a spectral calibration accuracy of ± 5 nm, Green[14] has shown that significant radiometric error is introduced with as little as ± 1 nm wavelength calibration error. This is due to the abundance of steep slopes and sharp absorption features in the terrestrial radiance spectra.

The two main sources of uncertainty in the laboratory calibration are the monochromator output wavelength versus counter position regression, and the center wavelength versus spectrometer channel regression. Table 7 shows the contribution to the maximum center wavelength accuracy for each AVIRIS spectrometer. This table can be used to bound the uncertainties in center wavelength for each of the 224 AVIRIS spectral channels.

In-flight verification of the spectral calibration uses atmospheric absorption features derived from a high-resolution LOWTRAN-7 model[15] as described by Green[16]. This technique shows agreement with the laboratory calibration at the ± 2-nm level.

Table 7. Spectral calibration error.

Spectrometer and spectral range (nm)	Maximum error due to monochromator calibration error (nm)	Maximum error due to spectrometer regression error (nm)
A 400 – 700	0.4	1.7
B 700 – 1200	0.9	0.3
C 1200 – 1800	0.9	0.4
D 1800 – 2450	0.6	1.3

5.2 Accuracy of the Radiometric Calibration

The absolute accuracy of the radiometric response function is estimated as the root sum square of the percent uncertainties in radiance of the integrating sphere and the system response to the integrating sphere. The integrating sphere radiance is shown in Figure 13 where the error bars indicate plus one to minus one sigma of uncertainty. The system response is shown in Figure 14 where error bars equal ± 1 standard deviations of the signal in DN during the calibration. The effects of these two uncertainty factors are RSS together to arrive at the calibration uncertainty in Table 8.

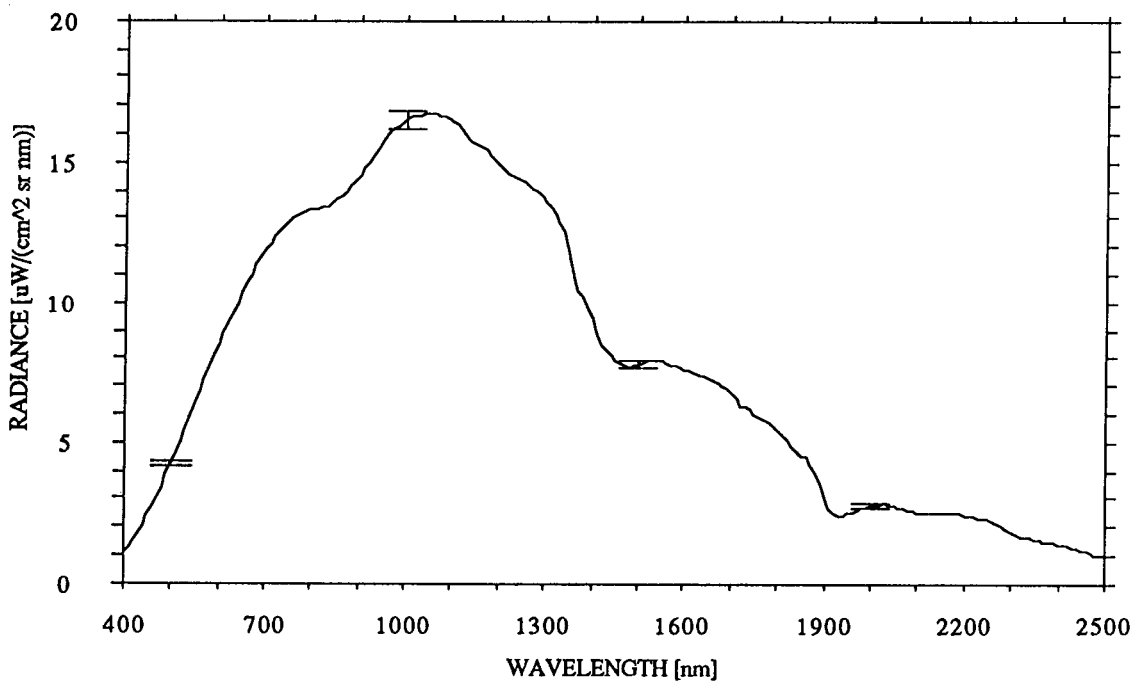

Figure 13. Integrating sphere radiance as a function of wavelength.

Table 8. Percent uncertainty of radiometric calibration.

Wavelength (nm)	Sphere Radiance (%)	Instrument Instability (%)	RSS Uncertainty (%)
500	1.50	2.87	3.24
1000	1.61	0.55	1.72
1500	1.78	0.62	1.96
2000	3.44	1.07	3.71

The percent instrument stability is bounded by the maximum minus the minimum divided by the average instrument response in DN to a constant source during a 2-hour period. Systematic changes in the instrument response between the laboratory and flight conditions are assessed using the in-flight calibration described by Green[17].

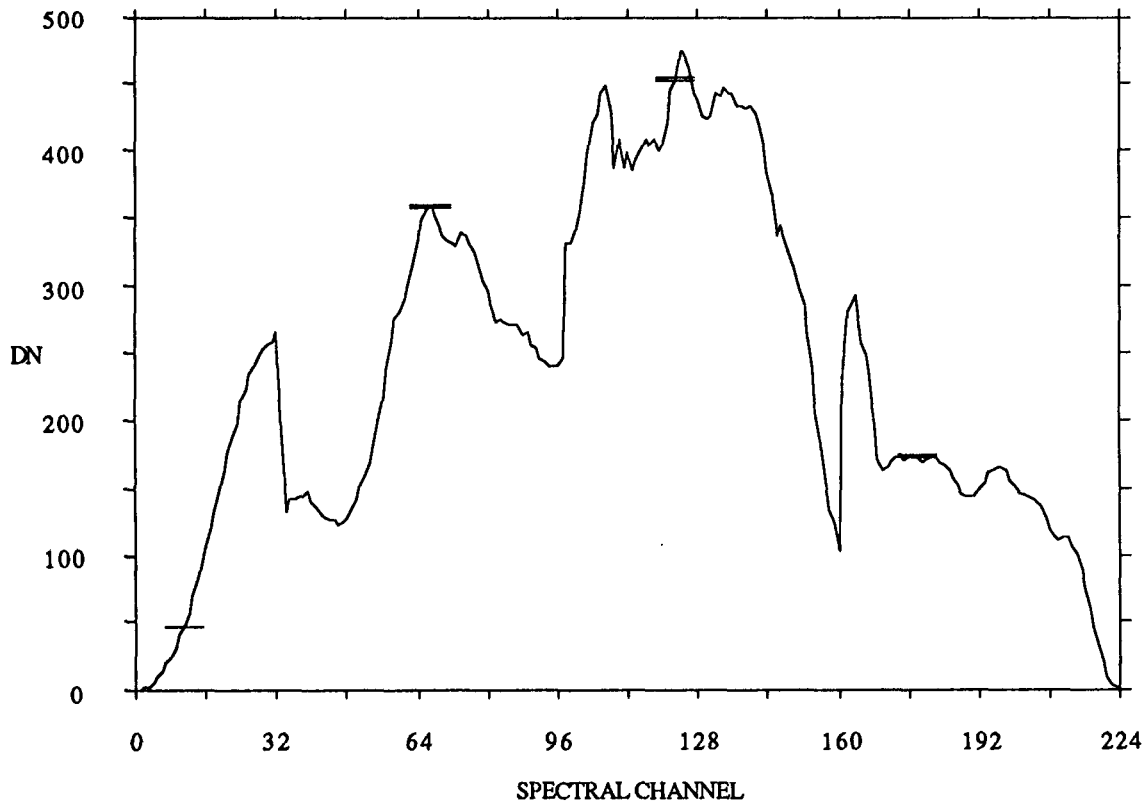

Figure 14. System response to integrating sphere as a function of spectral channel.

6.0 FUTURE PLANS

Future plans include the automation of spectral calibration in order to measure the spectral response function of all 224 channels. This will incorporate an automated monochromator calibration and a correction for intensity variations as a function of wavelength.

An investigation of the uncertainty of NIST (formerly NBS) standards of irradiance and spectral reflectance is also planned to improve the accuracy of the radiometric standards. Polarization and linearity data are currently being analyzed. Further intra- and interday stability tests are planned. A geometric performance assessment of AVIRIS will be repeated after a major refurbishment of the foreoptics and scan-drive mechanism planned for the winter of 1990.

The AVIRIS onboard calibration system, first described by Chrisp[18], has been modified during the spring of 1990. The modifications include a current stabilized power supply, a brighter lamp, and a new routing of the calibration signal. The new system uses a bundle of 32 fibers to illuminate the the backside of the foreoptics shutter. This allows the calibration signal to enter the spectrometer through the data fiber. The performance of these modifications will be closely monitored during the 1990 flight season and the results reported at a later date.

7.0 ACKNOWLEDGMENTS

The authors would like to express their thanks to the many members of the AVIRIS team who have helped to design, maintain, and improve the AVIRIS instrument and ground processing facility. The AVIRIS project is greatly indebted to them for the excellence of their contributions.

The work described in this paper was carried out at the Jet Propulsion Laboratory, California Institute of Technology, under a contract with the National Aeronautics and Space Administration.

8.0 REFERENCES

1. W. M. Porter and H. T. Enmark, "A system overview of the Airborne Visible/Infrared Imaging Spectrometer (AVIRIS)," Proc. SPIE, 834, (1987).

2. G. Vane, M. Chrisp, H. Enmark, S. Macenka, and J. Solomon, "Airborne Visible/Infrared Imaging Spectrometer: An advanced tool for earth remote sensing," Proc. 1984 IEEE Int'l Geoscience and Remote Sensing Symposium, SP215, 751-757 (1984).

3. G. Vane, T. G. Chrien, E. A. Miller, and J. H. Reimer, "Spectral and radiometric calibration of the Airborne Visible/Infrared Imaging Spectrometer (AVIRIS)," Proc. SPIE, 834, (1987).

4. W. M. Porter, T. G. Chrien, E. H. Hansen, and C. M. Sarture, "Evolution of the Airborne Visible/Infrared Imaging Spectrometer (AVIRIS) Flight and Ground Data Processing System," Proc. SPIE, 1298, (1990).

5. R. O. Green, J. E. Conel, J. S. Margolis, V. Carrere, C. J. Bruegge, M. Rast, and G. Hoover, "Inflight validation and calibration of the spectral and radiometric characteristics of the Airborne Visible/Infrared Imaging Spectrometer (AVIRIS), Proc. SPIE, 1298, (1990).

6. P. R. Bevington, Data Reduction and Error Analysis for the Physical Sciences, 169 pp., McGraw Hill, New York (1969).

7. S. A. Macenka and M. P. Chrisp, "Airborne Visible/Infrared Imaging Spectrometer (AVIRIS): Spectrometer design and performance," Proc. SPIE, 834, (1987).

8. H. Sobel, Gaussian fitting routine, AVIRIS design file 150 (JPL internal document).

9. Optronics irradiance standard report (Feb. 1, 1989), Optronics Laboratories, Inc., Orlando Fl.

10. Labsphere reflectance calibration certificate (June 01, 1988), Labsphere, Inc., North Hutton, NH.

11. Geophysical Enviromental Research Corp., Milbrook, NY.

12. J. H. Reimer, J. R. Heyada, S. C. Carpenter, W. T. S. Deich, and M. Lee, "AVIRIS ground data-processing system," Proc. SPIE, 834, (1987).

13. S. Larson, E. Hansen, and R. O. Green, "The AVIRIS data facility," Proceedings of the Second AVIRIS workshop, JPL publication (in press), (1990).

14. ibid 5.

15. F. X. Kneizys, E. P. Shettle, G. P. Anderson, L. W. Abrew, J. H. Chetynd, J. E. A. Shelby, and W. O. Gallery, Atmospheric Transmittance/Radiance; computer code LOWTRAN 7 (in press), AFGL Hanscom AFB, MA, 1989.

16. ibid 5.

17. ibid 5.

18. M. P. Chrisp, T. G. Chrien, and L. Steimle, "AVIRIS foreoptics, fiber optics, and on-board calibrator," Proc. SPIE, 834, (1987).